Magneto-Optical Response of Twisted Ferronematic Cells

V. I. Zadorozhnii[a]; K. V. Bashtova[a]; V. Yu. Reshetnyak[a]; T. J. Sluckin[b]

[a] Physics Faculty, National Taras Shevchenko University of Kyiv, Kyiv, Ukraine [b] School of Mathematics, University of Southampton, Southampton, United Kingdom

PLEASE SCROLL DOWN FOR ARTICLE

Taylor & Francis
Taylor & Francis Group

Magneto-Optical Response of Twisted Ferronematic Cells

V. I. ZADOROZHNII,[1] K. V. BASHTOVA,[1] V. YU. RESHETNYAK,[1] AND T. J. SLUCKIN[2]

[1]Physics Faculty, National Taras Shevchenko University of Kyiv, Kyiv, Ukraine
[2]School of Mathematics, University of Southampton, Southampton, United Kingdom

We construct a theoretical model for a thermotropic ferronematic (magnetic liquid crystal colloid) in an asymmetric twisted nematic cell, subject to in-plane magnetic fields. At low colloidal concentrations, the nematic director $\hat{n}$ is unchanged by strong fields, the magnetic director $\hat{m}$ principally responds to its coupling to $\hat{n}$, and the suspension density peaks sharply where $\hat{m}$ and H are co-aligned. At higher concentrations feedback between $\hat{m}$ and $\hat{n}$ aligns $\hat{n}$ over a significant part of the cell, and the suspension divides into a region where $\hat{n}$ is parallel to H, and a region where it is not. We also make calculations of the optical properties of this cell.

I. Introduction

Twisted and supertwisted nematic bistable films are widely used as electrically controllable light shutters in various liquid crystal displays. These devices depend for their operation on an electric Frederiks effect. The theory of this particular effect was in fact first discussed by Leslie [1] in the context of an ordering *magnetic* field, and follows the original experiments by Frederiks himself in the late 1920s [2]. But notwithstanding the early work of the pioneers, liquid crystal devices of the standard type which use magnetic rather electric ordering are almost unknown.

Magnetic-field-driven twisted nematic (TN) devices might be in more widespread use, were it not for the rather large value of the magnetic Frederiks threshold fields ($\sim 10^3$–10^4 Oe). However, it was proposed as long ago as 1970 [3] that doping liquid crystals with very low concentrations of submicron size ferromagnetic

particles would substantially increase the sensitivity of liquid crystal to weak magnetic fields. These hybrid materials can in principle be very sensitive to weak magnetic fields (<10 Oe) and would appreciably extend the functional possibilities of liquid crystal devices. A dramatic example of this phenomenon was observed by Chen and Amer [4]. A notable feature of these results is that the Frederiks threshold was eliminated. The results can be fitted to a theory by some of the present authors [5,6]. Although it has turned out to be difficult to reproduce the experimental results in ref. [4] in thermotropic liquid crystals, a related phenomenon seems to be rather readily accessible in lyotropic liquid crystals [7], albeit in concentrated colloidal samples.

Over the past decade, however, there has finally been further experimental progress in obtaining colloidal dispersions of ferroparticles in thermotropic liquid crystals (known usually as thermotropic ferronematics) which are stable towards ferroparticle coagulation [8]. This work has stimulated further theoretical research on the Frederiks effect in these materials [5,6]. This paper extends the theory of such devices developed in these papers to a simplified version of the twisted nematic geometry. Here we try to use parameters appropriate to sensible experimental situations to make explicit predictions.

Here we consider twisted ferronematic (FN) cells with walls whose easy axes are in-plane and mutually perpendicular. The nematic director anchoring at the ferroparticle surfaces is such that locally the magnetic and nematic directors prefer to be aligned. We present in this paper a model calculation in which the magnetic field is in specific the director plane. The anchoring strength is high on the lower and weak on the upper walls of the liquid crystal layer in the cell. This is a two-dimensional mimic of the more realistic case of hybrid anchoring, in which the boundary conditions on the walls are qualitatively different.

We show theoretical and simulation results for nematic and magnetic director reorientation in a magnetic field. With increasing magnetic field the nematic and magnetic directors tend to be oriented along the magnetic field. This tendency is opposed by anchoring forces at the walls of the cell. A consequence is that the ferroparticle density responds; the particles migrate to regions where the ferronematic coupling energy is minimized. To compare with possible experiment, we also investigate the resulting intensity and polarization state of the light reflected from and transmitted through the cell. Future work will consider more realistic twisted cells with a perpendicular field.

II. Model

The basic geometry of the problem is shown in Figure 1. The nematic and magnetic rotational distortions in an external magnetic field H are given respectively by the nematic director $\hat{\mathbf{n}} = [\cos\theta(z), \sin\theta(z), 0]$, and by the magnetic director $\hat{\mathbf{m}} = [\cos\psi(z), \sin\psi(z), 0]$ (i.e., unit vector in the direction of the sample magnetization). The easy axes at the two walls of the cell are mutually perpendicular ($\pi/2$ twist). The deviations of the nematic director from the easy axis at the lower and upper walls are θ_0, $\pi/2 - \theta_D$, respectively. Note also the angle α in the diagram indicating the direction of the magnetic field with respect to the easy direction at the lower wall. Magnetic particles are rod-like magnetic grains in the single-domain state, with magnetic moment aligned along the long axis of the grain.
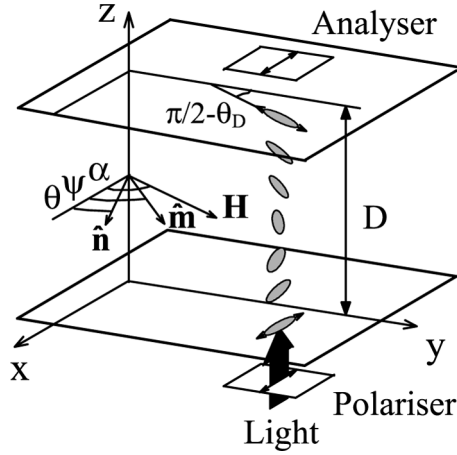
Figure 1. Schematic of the FN cell.

FN equilibrium configurations at a given magnetic field are obtained by minimizing the free energy functional (see [9]):

$$F = \int_V \left\{ \frac{1}{2} [K_1 (\nabla \cdot \hat{\mathbf{n}})^2 + K_2 (\hat{\mathbf{n}} \cdot \nabla \times \hat{\mathbf{n}})^2 + K_3 (\hat{\mathbf{n}} \times \nabla \times \hat{\mathbf{n}})^2] - \frac{1}{2} \chi_a (\hat{\mathbf{n}} \cdot \mathbf{H})^2 \right.$$
$$\left. - M_S f (\hat{\mathbf{m}} \cdot \mathbf{H}) - 2f \frac{W_p}{d} (\hat{\mathbf{n}} \cdot \hat{\mathbf{m}})^2 + \frac{f k_B T}{v} \ln f \right\} dV$$
$$+ \frac{1}{2} W_0 \sin^2(\theta_0) + \frac{1}{2} W_D \sin^2(\pi/2 - \theta_D), \tag{1a}$$

where K_1, K_2 and K_3 are the (Frank) elastic constants, χ_a is the anisotropy of the nematic diamagnetic susceptibility, M_S is the saturation magnetization within an individual colloidal particle, $f = cv$ is the local volume particle fraction, v is the colloidal particle volume, c is the magnetic colloid concentration, W_p is the soft planar anchoring energy of the colloidal particle due to the nematic-ferroparticle surface interaction, W_0 and W_D are the anchoring energies at the lower and upper walls respectively, T is absolute temperature and k_B is Boltzmann's constant.

The minimization is carried out subject to the constraint of ferroparticle number conservation:

$$\int f \, dV = \bar{f} V, \tag{1b}$$

where $\bar{f}$ is the mean ferroparticle fractional volume concentration. Finally, we note that in this calculation, the anchoring at the lower wall is strong, and the anchoring at the upper wall is weak, i.e., $W_0 \gg W_D$.

A number of different non-dimensional schemes have been proposed to reduce the number of parameters in this problem [9,5,6]. For this paper, we have used the scaling discussed by [9], and the same numerical techniques used in refs. [5,6], which will be discussed in more detail elsewhere [10].

III. Numerical Results

To make contact with possible experiment, we have used the following quantities in our numerical estimates (See Table 1).

In the first two examples, we suppose that $\alpha = \pi/8$, i.e., the bulk magnetic field is closer to the easy direction of the strongly anchored wall. In the first example, we suppose a *very* low ferroparticle fractional volume concentration of $\bar{f} = 3.5 \times 10^{-6}$. The results are shown in Figure 2.

The key points to note are that the low ferroparticle concentration is such that the ferroparticles are affected by the magnetic field, but the nematic director is unaffected, as can be seen in Figure 2(a). It remains linear as a function of distance, no matter the strength of the field (the direct effects are weak). In Figure 2(b), the magnetic director, by contrast, can be seen to be a compromise between the effect of the nematic director (which does act strongly on it, although the effect is not mutual) and the easy bulk direction. The result is that the magnetic director is also linear with distance. There is a "sweet spot," closer to the strong anchoring wall, at which the magnetic director is invariant. This occurs when the unperturbed nematic director lies along the bulk magnetic direction. For high fields, the system prefers the magnetic director to lie in this direction, and hence the magnetic particles should migrate

Table 1. Quantities in numerical estimates

Cell	$D = 50\,\mu m$
Anchoring at lower wall	$W_0 = 0.1\,erg/cm^2$
Anchoring at upper wall	$W_D = 5 \times 10^{-4}\,erg/cm^2$
Anchoring at the particle surface	$W_P = 3.7 \times 10^{-2}$
Magnetic particle length	$L = 0.2\,\mu m$
Magnetic particle width	$d = L/3$
Saturation magnetization of magnetic material	$M_S = 485\,G$ (Fe$_3$O$_4$)
Liquid crystal properties	5CB ($T = 25°C$)
Frank-Oseen twist elasticity	$K_2 = 4.1 \times 10^{-7}\,dyn$
Anisotropic part of diamagnetic susceptibility	$\chi_a = 1.7 \times 10^{-7}$
Ordinary refractive index ($\lambda_{Light} = 514.5\,nm$)	$n_o = 1.5442$
Extraordinary refractive index	$n_e = 1.7360$
Dimensionless magnetic field h	$h = M_S v H / k_B T$
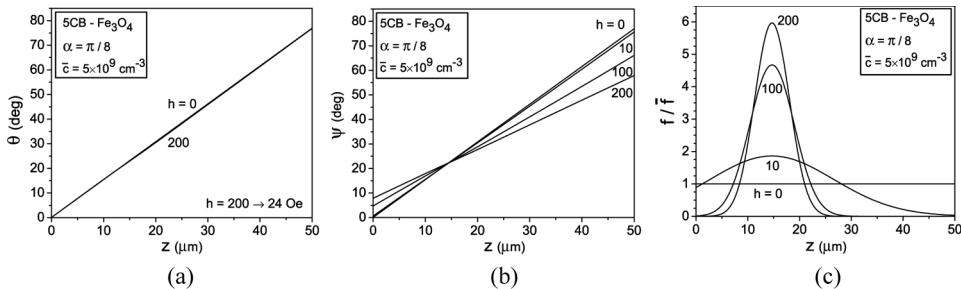
Figure 2. FN director and ferroparticle profiles, $\alpha = \pi/8$, $\bar{f} = 3.5 \times 10^{-6}$ (low ferroparticle concentration). See discussion in text, noting the "sweet spot" close to $z = 15\,\mu m$, $\psi = \alpha = \pi/8$.
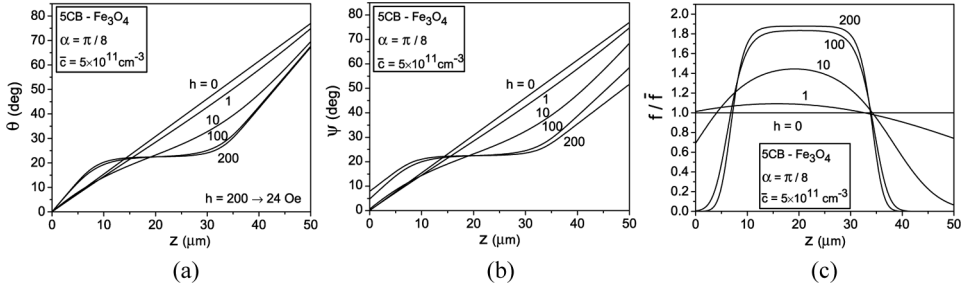
Figure 3. FN director and ferroparticle profiles, $\alpha = \pi/8$, $\bar{f} = 3.5 \times 10^{-4}$ (high ferroparticle concentration). See discussion in text. The "sweet spot" close to $z = 15\,\mu$m, $\psi = \alpha = \pi/8$ is broadened into a wide region, thus weakening the magnetic segregation.

toward this region. This can be seen in Figure 2(c); for dimensionless field $h = 10$ the effect is noticeable but minor, with $f_{max}/\bar{f} \sim 2$. But by the time $h = 200$, this ratio has reached 6, the magnetic particles are well-localised close to the "sweet spot," and very few magnetic particles can be found in the half of the cell where the magnetic director would point well away from the magnetic field. But even in the high field limit, there is no feedback to the nematic director behavior.

In Figure 3, we consider the same situation, but now the ferroparticle volume fraction is increased a hundred-fold to $\bar{f} = 3.5 \times 10^{-4}$. This still seems like a very low concentration, but in fact it is now sufficient, at least in theory to give significant magnetic-nematic feedback. Now the linear spatial dependence of nematic director on field is significantly affected by the field. Now at least at high fields, there is a significant region over which the bulk magnetic field "wins" entirely, in the sense that in this region the magnetic director points along the magnetic field, and the nematic-magnetic coupling reorients the nematic director in this region as well. The "sweet spot" is thus broadened. But paradoxically, the magnetic segregation effect (in some sense the most dramatic effect here) is *weakened*. For because there is a whole region, and not just a "spot" over which the magnetic director is aligned with the bulk field, there is a whole region over which the magnetic director can align and still minimise the free energy. The result is that the ferroparticle profile is no longer approximately Gaussian (as it was in the low concentration case), but rather square, and divided into wide "good" and "bad" regions. The finite width of the good regions means the maximum value $f_{max}/\bar{f}$ is much lower than in the low concentration case.
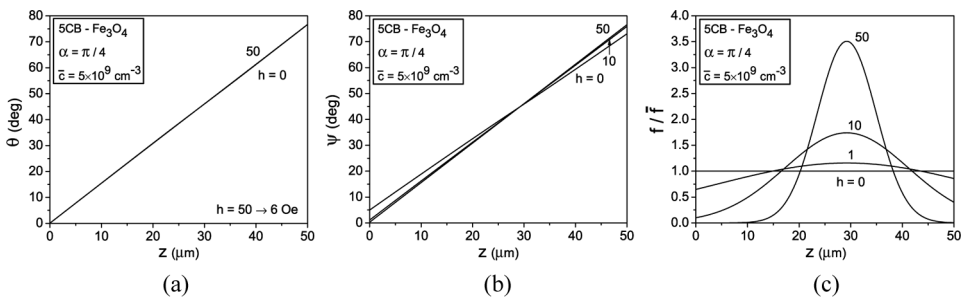
Figure 4. Low ferroparticle concentration, as for Figure 2, but with $\alpha = \pi/4$. See discussion in text, noting movement of "sweet spot" as compared to Figure 2.
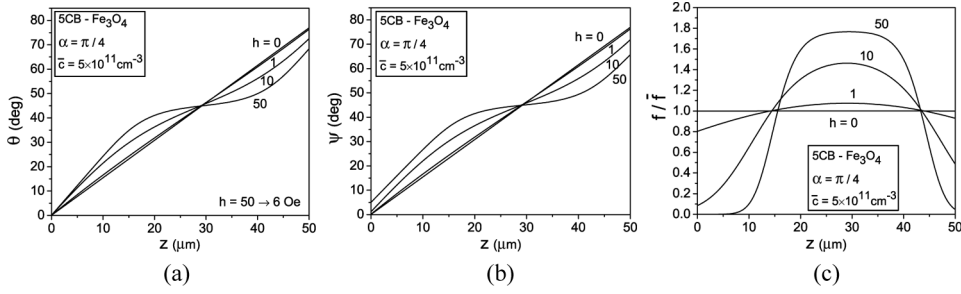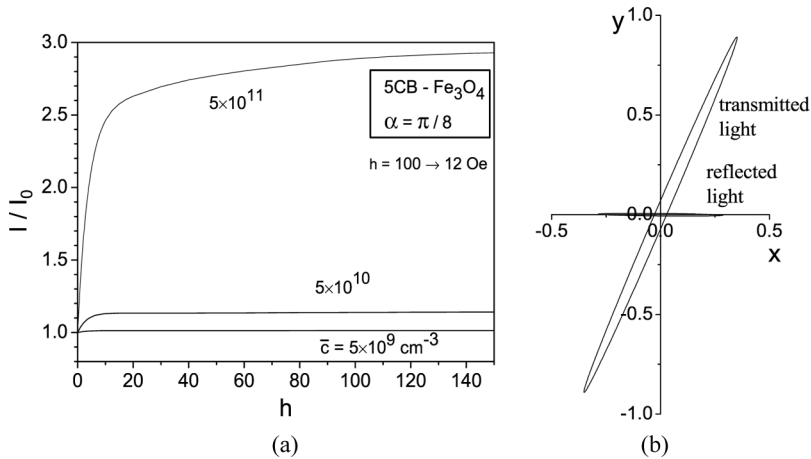
Figure 5. High ferroparticle concentration, as for Figure 3, but with $\alpha = \pi/4$. See discussion in text, noting movement of "sweet region" as compared to Figure 3.

Similar features can be observed for $\alpha = \pi/4$. The "sweet spot" is now closer to the centre of the sample (approximately 0.6 of the way across the sample). The movement of the "sweet spot" is a consequence of the fact that the easy bulk direction and the unperturbed direction of the nematic director will necessarily move across the sample as α increases. These results are shown in Figure 4 (low ferroparticle concentration), and Figure 5 (high concentration).

IV. Magneto-Optic Response

In order to make contact with experiment, we have also made calculations of the optical signature of this system when placed between polariser and analyser, using the Berreman 4×4 matrix method [11,12]. Some results, for the cases considered above, are shown in Figures 6 and 7.

Figure 6. (a) Magneto-optic response in a $\pi/2$-twist ferronematic cell at different ferroparticle concentrations. $\alpha = \pi/8$. I_0 is the intensity of light transmitted through the cell at $H = 0$. (b) Polarization states for transmitted and reflected light at $\bar{c} = 5 \times 10^{11}\,\mathrm{cm}^{-3}$ and $h = 150$. The incident light is polarized along the x-axis, i.e., parallel to the easy axis of the lower wall.
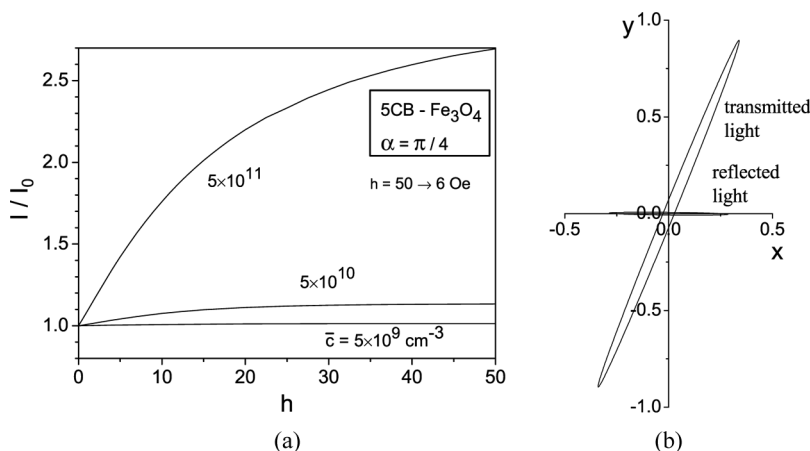
Figure 7. (a) Magneto-optic response with $\pi/2$-twist. As for Figure 6, but with $\alpha = \pi/4$. (b) Polarization states for transmitted and reflected light at $\bar{c} = 5 \times 10^{11}\,\mathrm{cm}^{-3}$ but now $h = 50$. Polarisation of incident light as in Figure 6.

V. Conclusions

We have analysed the behavior of a twisted ferronematic system in an external magnetic field. In this model at the lower wall of the liquid crystal cell the nematic anchoring is strong, but at the upper wall it is weak, and we suppose that the ferro-particles tend to align parallel to the magnetic field. We have also investigated the intensity and polarization state of light reflected from and transmitted through the cell for different particle concentrations as a function of magnetic field strength.

With increasing magnetic field applied parallel to the cell walls the nematic and magnetic directors tend to be oriented along the magnetic field. This tendency is opposed by anchoring forces at the walls of the cell. The magnetic particle density responds so that particles migrate to regions where the ferronematic coupling energy is minimized. The concentration of particles has a maximum in the region of co-alignment of the nematic director $\hat{n}$ and H. Our preliminary numerical simulations show that in the twisted FN cell an additional strong direct magnetic field can cause the twisted configuration to unwind. In particular, we predict a noticeable decrease in the unwinding threshold as compared to the pure TN cell.

In principle this system is very highly magnetically sensitive. There are numerous possible applications, if suitable cells can be prepared. A non-exclusive list might include magnetic sensors, magnetic field-controlled devices for processing, and information storage. The geometry (though not the field configuration) discussed here, with different anchoring strengths at opposite cell walls, has been discussed by Dozov et al. [13] in the context of a switchable bistable cell. The present calculation suggests the prospect of a magnetically switchable bistable liquid crystal device. In future work we shall discuss the more realistic case when the magnetic field is normal to the walls of the cell.

Acknowledgments

References

[1] Leslie, F. M. (1970). *Mol. Cryst. Liq. Cryst.*, *12*, 57.

[2] Freedericksz, V., & Zolina, V. (1929). *Trans. Am. Electrochem. Soc.*, *55*, 85–96. [Reprinted in T. J. Sluckin, D. A. Dunmur, & H. Stegemeyer (Eds.). *Crystals that Flow*, Taylor and Francis, 222–233 (2004).]

[3] Brochard, F., & de Gennes, P. G. (1970). *J. Physique (France)*, *31*, 691.

[4] Chen, S.-H., & Amer, N. M. (1983). *Phys. Rev. Lett.*, *51*, 2298.

[5] Zadorozhnii, V. I., Vasilev, A. N., Reshetnyak, V. Yu., Thomas, K. S., & Sluckin, T. J. (2006). *Europhys. Lett.*, *73*, 408.

[6] Zadorozhnii, V. I., Sluckin, T. J., Reshetnyak, V. Yu., & Thomas, K. S. (2008). *SIAM J. Appl. Math.*, *68*, 1688.

[7] Lemaire, B. J., Davidson, P., Ferré, J., Jamet, J. P., Panine, P., Dozov, I., & Jolivet, J. P. (2002). *Phys. Rev. Lett.*, *88*, 125507.

[8] See e.g., Buluy, O., Ouskova, E., Reznikov, Yu., & Litvin, P. (2004). *Ukr. J. Phys.*, *49*, N12A, A48.

[9] (a) Burylov, S. V., & Raikher, Yu. L. (1995). *Mol. Cryst. Liq. Cryst.*, *258*, 107; (b) *ibid. 258*, 123.

[10] Zadorozhnii, V. I., Bashtova, K. V., Reshetnyak, V. Yu., & Sluckin, T. J. Poster ID-532, 23rd International Liquid Crystal Conference, Kraków.

[11] Berreman, D. W. (1975). *J. Appl. Phys.*, *46*, 3746.

[12] Wöhler, H., Haas, G., Fritsch, M., & Mlynski, D. A. (1988). *J. Opt. Soc. Am. A*, *5*, 1554.

[13] Dozov, I., Nobili, M., & Durand, G. (1997). *Appl. Phys. Lett.*, *70*, 1170.